Preparation of Magnetic Nanospheres from a Reverse Microemulsion Stabilized by a Block Copolymer Surfactant

Zhiming Chen, Zhen Jiao, Zhiqiang Li

School of Chemistry and Chemical Engineering, Southeast University, Nanjing 210096, People's Republic of China

Received 7 March 2007; accepted 10 January 2008
DOI 10.1002/app.28088
Published online 28 July 2008 in Wiley InterScience (www.interscience.wiley.com).

ABSTRACT: A new method for the preparation of magnetic nanospheres is reported. It involved the dispersion of an aqueous phase containing Fe^{3+}, Fe^{2+}, or/and Ni^{2+} ions into droplets in an organic medium with an amphiphilic block copolymer, which was synthesized through atom transfer radical polymerization at a lower temperature (70°C) and was then sulfonated by sodium hydrogen sulfite in tetrahydrofuran as a surfactant. A reduction was carried out in the water pool as a microreactor, which resulted in the yielding of polymer/magnetite particles. The size of the prepared spheres could be tuned up by variation of the preparation conditions, including the stirring speed, copolymer content, and so on. The average diameter was homogeneous and was about 10 nm. The magnetic nanospheres, whose saturation magnetization of magnetic nanoparticles of 3.8×10^{-3} emu/g was less than their bulk counterparts, exhibited characteristics of superparamagnetism. © 2008 Wiley Periodicals, Inc. J Appl Polym Sci 110: 1664–1670, 2008

Key words: atom transfer radical polymerization (ATRP); block copolymers; magnetic polymers; microencapsulation; nanocomposites

INTRODUCTION

Magnetic nanospheres display magnetic properties different from their bulk material counterparts. These unique properties originate from the sizes of the particles, which are below a critical diameter for magnetic domain wall formation. In the absence of an externally applied magnetic field, thermal energy can be sufficient to cause the magnetic moments in these single-domain particles to equilibrate and overcome any preferential orientation. However, when the particles are placed in an external magnetic field, their magnetic moments align rapidly in the direction of the field and the materials display a net magnetization. When the magnetic field is removed, the thermal energy is again sufficient to cause the particles' vector moments to fluctuate randomly. The magnetization of the magnetic nanosphere investigated in this study disappeared when the external field was removed (i.e., they had near-zero magnetic remanence and coercivity) in a short while relative to the experimental time. These properties indicated superparamagnetic behavior of the magnetite nanosphere, which suggests that it may be ideal for components of vehicles for magnetic-field-directed delivery of therapeutic agents.

Magnetic nanospheres can be dispersed in carrier fluids through specific interactions between the particle surfaces and selected low-molecular-weight or polymeric surfactants. Such fluid dispersions of small magnetic particles are known as *ferrofluids*.[1] Magnetic attractive forces combined with inherently large surface energies (>100 dyn/cm)[2] can favor nanosphere aggregation in magnetic dispersions.[1,3] Thus, the properties of the surfactants and the nature, as well as the concentration, of binding sites between surfactants and the particle surface are important for obtaining good dispersion (without particle aggregation).

The current and potential applications for magnetic nanomaterials in electronics and biotechnology are diverse. Nanomagnetic films have great promise for electronic and electrical devices, sensors, electromagnetic shielding, and high-density digital storage.[4] Biomedical applications under current investigation include retinal detachment therapy,[5] cell separation methods,[6,7] tumor hyperthermia,[8] improved MRI diagnostic contrast agents,[2,9–11] and magnetic-field-guided carriers for localizing drugs or radioactive therapies.[12–14]

The nanosphere surface can influence material durability in biological environments. These particles must remain nonaggregated, be stable against oxidation, and display high magnetization during applications. Transition metals can offer high magnetization;

Correspondence to: Z. Chen (chenzm@seu.edu.cn).
Contract grant sponsor: Southeast University Foundation.
Contract grant sponsor: Jiangsu Hightech Project; contract grant number: BG2006038.

unfortunately, they are sensitive to oxidation, which results in a loss of magnetic response because of the formation of antiferromagnetic oxides. Currently, oxidization of the transition metals remains a hurdle, especially in biomedical, oxygen-rich environments. Iron oxides, such as magnetite (Fe_3O_4) and maghemite (γ-Fe_2O_3), are more stable against oxidation. These materials can be formed at low temperatures and under mild conditions and display strong ferrimagnetic behavior. In addition, previous investigations have shown that magnetite has high LD_{50} (the dose that will kill 50% of the tested group) values (LD_{50} in rats = 400 mg/kg) and polymer-coated magnetite has not shown any acute or subacute toxicity in animal studies.[15]

Magnetite particles are commonly prepared by the condensation of divalent and trivalent iron salts reacted with hydroxide bases (pH = 9.5–10). The magnetite crystal structure forms readily in aqueous media. Methods to prevent agglomeration include the use of electrostatic and steric (entropic) stabilizers. Aqueous dispersions have been reported with electrostatic stabilizers,[16] bilayer surfactants,[17–20] polymers as steric stabilizers,[21–26] and polymer templates.[27] Many of the reported stabilizers were not designed with functional groups to bind to the magnetite surface, and thus, their dispersion stability was limited.

The microemulsion method has been used to control polymer morphologies. In this article, we report the preparation of amphiphilic diblock copolymers containing controlled concentrations of sulfonic groups (—SO_3H) in the segments of poly(butyl methacrylate)-*block*-poly(glycidyl methacrylate) (P(BMA-*b*-GMA)). A method for the preparation of magnetite nanospheres and subsequent stabilization and dispersion with these polymers is described. The reverse microemulsion consisted of aqueous domains dispersed in a continuous oil phase. Under appropriate conditions, a variety of reactants could be introduced into the nanosized aqueous domains for reaction, which led to materials with a controlled size and shape. These small aqueous domains could be viewed as nanoreactors for the synthesis of magnetic nanospheres. The resultant polymer-coated magnetite nanosphere was 10 nm in diameter. They were dispersible in both water and organic solvents, both of which were good solvents for P(BMA-*b*-GMA). These dispersions were stable in pH ranges common for biological systems and at the isoelectric point of uncoated magnetite (pH $\approx$ 6.8).[1] The microemulsion synthesis theme is schematically illustrated in Figure 1.

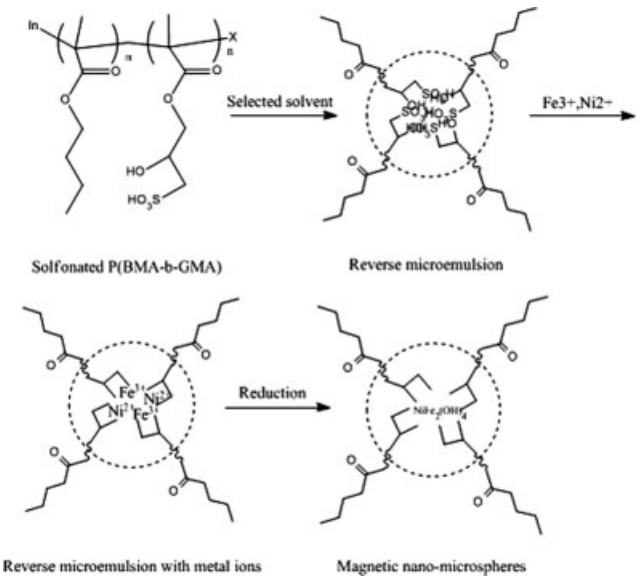

Figure 1 Preparation of the magnetic nanospheres.

EXPERIMENTAL

Preparation of the block copolymer

Polymerization was carried out with Schlenk techniques under an argon atmosphere. To a dry, 10-mL, round-bottom Schlenk flask with a magnetic stirring bar, the solvent 4-methy-2-pentanone (which could make the initiator dissolve to obtain homogeneous system to result in a more rapid reaction), the ligand (Phen), Cu, and $CuCl_2$ were added. After that, the flask was closed with a stopcock. The contents of the flask were then placed *in vacuo*, and the flask was backfilled with argon three times to remove oxygen. The degassed monomer and solvent were then added by a syringe. After the mixture was stirred at room temperature until it was homogeneous, the initiator *p*-methyl benzenesulfonyl chloride was added, and the flask was immersed in a water bath kept at the desired temperature.

After some minutes, the second monomer was directly added. At timed intervals, some samples, which were used for the determination of percentage monomer conversion and molecular weight by gas chromatography and gel permeation chromatography, respectively, were withdrawn via syringe and diluted with tetrahydrofuran (THF).

Finally, the flask was removed from the water bath, and the mixture was diluted with THF. The solution was passed over a column with neutral alumina to remove the catalyst, after which the remaining solution was concentrated by rotary evaporation; the product was then dried at 60°C *in vacuo*.

Sulfonation of the block copolymer

Sulfonation was carried out according to the procedure described by Kim et al.[28] In an agitated reactor, the polymer was dissolved in THF at 40–60°C. Then, a water solution of sodium hydrogen sulfite was added under stirring. Samples were

removed at the desired reaction time intervals and precipitated in methanol or deionized water (1 L/10 g of polymer used). The highly sulfonated polymer was partially soluble in methanol or water, which was recovered by steam stripping and vacuum-dried at 80–90°C for a few days.

The complete removal of residual acid from the final product after sulfonation was important because it could interfere with the properties of the final product. The dried polymer was washed once with boiling deionized water and then washed many times with cold water until a neutral pH of the sewage was obtained. It was finally vacuum-dried at 80–90°C for the last time.

The titration of the polymer against a standard potassium hydroxide solution (0.1*N*) with phenolphthalein as an indicator showed a sulfonation level higher than 90%. The sulfonated polymer structure was characterized by Fourier transform infrared (FTIR) spectroscopy.

Preparation of the magnetic nanopolymer

Magnetite was produced according to a literature method.[29] Nickel, zinc, and manganese ferrites nanospheres were synthesized with the reverse microemulsions, which were spheroidal aggregates formed when the sulfonated block polymer was dissolved in a selected organic solvent. They were both formed with and without water. If the medium was completely free of water, the aggregates were very small and polydisperse. Otherwise, they were readily solubilized in the polar core and formed a so-called water pool, which was characterized by the water/surfactant molar ratio. The aggregates containing small amounts of water were called *reverse micelles,* whereas the microemulsions corresponded to droplets containing a large amount of water molecules.[30] The reverse microemulsion was first produced to carry out a reaction within it. They were obtained by the rapid agitation of the polymer and selected organic solvent, which was defined as the *primary microemulsion.* Then, the primary microemulsion was divided into two halves and added to the aqueous solutions of the reactant salts [iron sulfate and metal (Ni, Zn, Mn) sulfate] and the precipitating agent (NH_4OH). Thus, two microemulsions were made, one consisting of the reactant sulfate salts inside the reverse microemulsion (I) and the other consisting of the precipitating agent inside the reverse microemulsion (II). The two microemulsions were mixed and subjected to rapid mechanical stirring. The reverse microemulsion present in the organic phase moved around in the entire volume of the organic phase in a random Brownian motion. As a result, they collided with each other. These collisions resulted in the fusion of two reverse micelles to form a transient dimer. The dimer had a very short life, and it broke again into two reverse micelles with contents from one reverse micelle completely transferred into the other. The collisions might have also resulted in the diffusion of the contents from one reverse micelle into the other. In both cases, we obtained a system with both the reactants and the precipitate in the same reverse microemulsion. After a precipitation reaction, metal ferrite was obtained.

The reactant salt solution was composed of hydrated iron sulfate and hydrated metal sulfate (nickel, zinc, or manganese sulfate) in stoichiometric quantities according to the product, that is, for MFe_2O_4 (i.e., [Fe2+]/[M2+] = 2). In microemulsion II, ammonium hydroxide was the precipitating agent. The two microemulsions were subjected to rapid mechanical stirring for 30 min. The metal hydroxides were precipitated within the water pools of the reverse micelles and oxidized to ferrite. The precipitation of ferrite occurred according to the following reaction:

$$MSO_4 \cdot 6H_2O + 2FeSO_4 \cdot 7H_2O + 6NH_4OH + 12O_2 \rightarrow MFe_2O_4 \downarrow + 16H_2O + 3(NH_4)_2SO_4$$

After rapid mechanical stirring, methanol was added to the resulting mixture to extract the polymer and the organic selected solvent. The resulting liquid was separated by a centrifuge, and the ferrite product was washed with a lot of methanol. The solid particles contaminated with the polymer were settled down in the solution. The ferrite was then dried in an oven at 100°C. Morphology characterization of the ferrites was carried out with transmission electron microscopy (TEM). The magnetic properties of the ferrites were characterized by vibrating sample magnetometry in terms of the effect of applied field on magnetization.

RESULTS AND DISCUSSION

Preparation of the well-defined block copolymer

We monitored the kinetics and molecular weight growth of the polymerization of butyl methacrylate (BMA) and glycidyl methacrylate (GMA) by periodically removing samples from the reaction mixture and then analyzing them with the help of gel permeation chromatography and gas chromatography. The experimental data of the atom transfer radical polymerization (ATRP), including the reaction temperature, the number-average molecular weight, the molecular weight distribution of the polymer, and conversion, are presented in Table I.

Some research indicated[31] that with increasing reaction temperature, the rate of polymerization increased, whereas the ratio of rate constant for propagation/rate constant for radical termination

TABLE I
ATRP Results of BMA and GMA at Different Temperatures

Temperature (°C)	$M_{n,sec}$	M_w/M_n	Conversion (%)
70	12,300	1.07	80
75	14,900	1.18	87
80	15,680	1.22	89
90	16,750	1.27	90

M_w, weight-average molecular weight; M_n, number-average molecular weight.

(k_t/k_p) descended; then the termination reactions would be controlled. Furthermore, from these data, we found that it can improve the efficiency of initiation when the temperature rises, but the molecular weight distribution also becomes wide. The reason is that the diradical termination reactions clearly increase in the system, then large numbers of irreversible copper(II) are generated, and as a result, the reaction cannot be well controlled. So reactions with a low temperature and long time are better for obtaining copolymers with a narrow distribution for the ATRP reaction. According to our study, the optimal temperature and reaction time were 70°C and 12 h, respectively.

Figure 2 shows the kinetic plot of the ATRP of BMA and GMA at different temperatures. The monomer conversion increased gradually along with the extension of reaction time. Also, the reaction rate increased linearly with time; in other words, the relation between the apparent reaction rate and monomer concentration conformed to first-order reaction kinetics. So the living polymerization came true, and the concentration of the propagating chain free radical remained at a constant quantity in polymerization. The rate laws were derived as follows:

$$R_p = -\frac{d[\mathrm{M}]}{dt} = k_p[\mathrm{P}\cdot][\mathrm{M}] = k_p K_{eq}[\mathrm{In}]\frac{[\mathrm{Cu(I)}]}{[\mathrm{Cu(II)X}]}[\mathrm{M}] \quad (1)$$

$$K_{eq} = \frac{k_{\mathrm{act}}}{k_{\mathrm{deact}}} = \frac{[\mathrm{P}\cdot][\mathrm{Cu(II)X}]}{[\mathrm{Cu(I)}][\mathrm{PX}]} \quad (2)$$

where R_p is the propagation rate, [M] is the monomer concentration, t is time, [P·] is total radical concentration, [In] is initiator concentration, [Cu(II)X] is concentration of Cu(II) chloride, [PX] is concentration of polymer chloride, K_{eq} is equilibrium constant for exchange reaction, k_{act} is rate constant for activation, k_{deact} is rate constant for deactivation, [P_i] is concentration of active chain with length i, [P_iX] is concentration of poly chloride with chain length i, $[\mathrm{M}]_0$ is initial concentration of monomers, k_p^{app} is appearance rate constant for propagation, and R_t is bimolecular termination reaction rate.

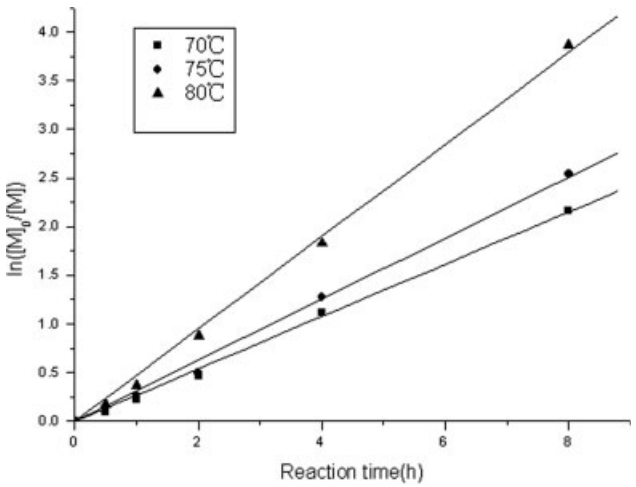

Figure 2 Kinetic plot of the ATRP of BMA and GMA at different temperatures.

where [In] = [PX], $[\mathrm{P}\cdot] = \sum_{i=1}^{\infty}[\mathrm{P}_i^{\cdot}]$, and $[\mathrm{PX}] = \sum_{i=1}^{\infty}[\mathrm{P}_i\mathrm{X}]$. If [P·] is constant

$$\ln\left(\frac{[\mathrm{M}]_0}{[M]}\right) = k_p[\mathrm{P}\cdot]t = k_p{}^{\mathrm{app}}t \quad (3)$$

In addition

$$\frac{R_t}{R_p} = \frac{k_t[\mathrm{P}\cdot]}{k_p[\mathrm{M}]} \quad (4)$$

According to eqs. (1) and (4), R_t/R_p would increase when the monomer concentration decreased, which would result in an increase in radical combination termination. Then, the molecular weight distribution would become wide. Thus, it was not suitable because it would prolong the reaction time to an excessive degree. By our experiments, the optimal reaction temperature and time were 70°C and 12 h, respectively, for higher conversion and with a resulting copolymer with a narrow distribution for by ATRP.

Sulfonation of the block copolymer

In terms of the sulfonation reaction, the polarity of the solvent dissolving the polymer is one of the most important factors. As shown in Table II, if the solvent's polarity was strong, just as for dimethylfor-

TABLE II
Effect of the Kind of Solvent on Sulfonation

Solvent	THF	Benzene	DMF	Cyclohexane
Sulfonation degree	91%	10.5%	7.6%	0

The reaction time was 8 h, and the temperature was 50°C.

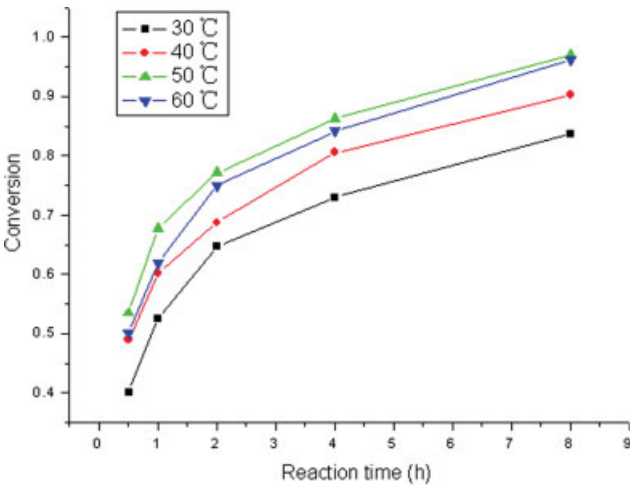

Figure 3 Conversion of sulfonation at different temperatures. [Color figure can be viewed in the online issue, which is available at www.interscience.wiley.com.]

mamide (DMF), it could integrate with water at first when the sulfonation agent water solution was added and lead the polymer to separate out from the system during the reaction, which resulted in it being more difficult for the polymer to collide and react with both of the reactants; then, the sulfonation rate was low. On the contrary, the polymer would not dissolve in the solvent whose polarity was too weak. Thus, THF, whose solubility parameter was close to the value of the polymer, was a suitable solvent.

Figure 3 compares the conversion of the sulfonation at different temperatures. The figure indicates that the conversion increased along with the reaction time. The reason is that epoxy group was embedded in the polymers in the reaction system. Furthermore, the long chain had stronger steric hindrance. So the reaction carried through gradually, and the reaction time was prolonged for a higher conversion.

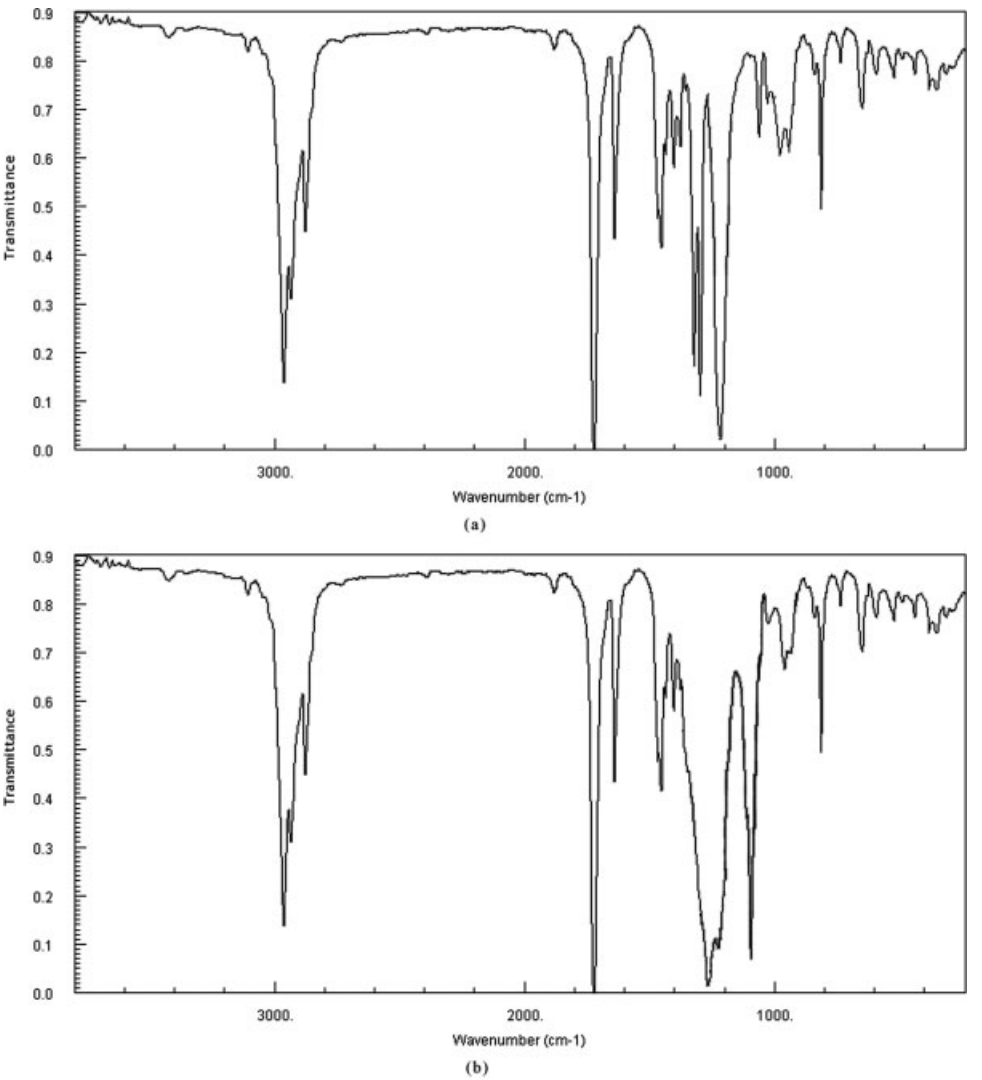

Figure 4 FTIR diagrams of the block copolymers before and after sulfonation.

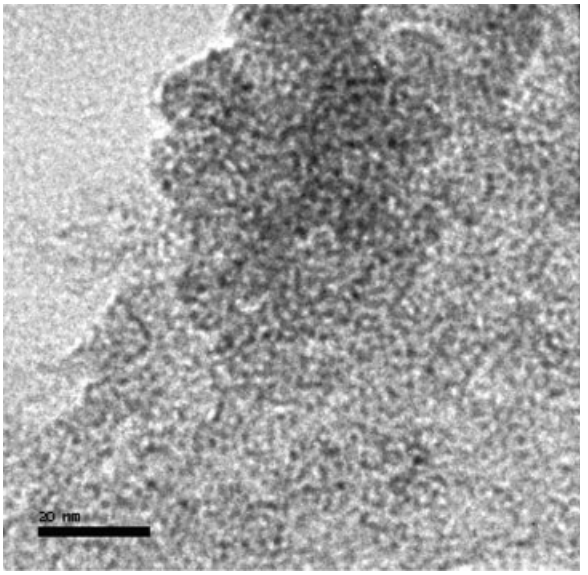

Figure 5 TEM image of a magnetite sample.

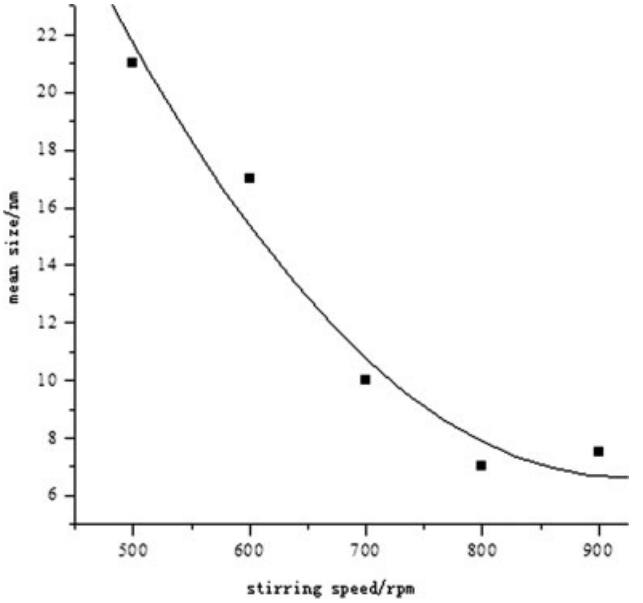

Figure 6 Effect of the stirring speed on the particle size.

Temperature was another factor in this reaction. A higher temperature was beneficial for the open-loop reaction of the epoxy group, which made the movement of ion-exchange equilibrium faster, lowered the steric hindrance, and then increased the contact chance between the chain and the sulfurous acid group, which led to an increase in the conversion. However, when the temperature reached 60°C, the system lost solvent fast, even in the reflux condition, which led more polymer to be separated from the system, and the temperature as a stimulus was weakened; then, the conversion dropped off.

The structure of the polymer samples before and after sulfonation was characterized by FTIR. The results are given in Figure 4. The FTIR diagram of the block polymer P(BMA-*b*-GMA) and the sulfonated polymer are given in Figure 4(a,b). All characteristic adsorption peaks of the epoxy group at 1239.46, 970.40, and 765.92 cm^{-1} are present in Figure 4(a). Nevertheless, these adsorption peaks disappeared in Figure 4(b), whereas the characteristic adsorption peaks of the sulfonation group appeared. This proved that the epoxy group was really transformed into the sulfonation group.

Morphology and characterization of the magnetic nanopolymer

Figure 5 shows a typical TEM image of the nanospheres' morphology and complex microconstruction. The average diameter was about 10 nm by calculation. Microspheres were in a single particle state and presented a polyphase structure of nucleus and shell. The surface of the microsphere was lipophilic PBMA, which was light, and the interior was the metallic oxide embedded by hydrophilic sulfonated PGMA, which was dark. The spheres had good uniformity. The surface shape of dysphasia was irregular because the metallic oxides did not crystallize in the reaction.

The system that we studied involved the use of sulfonated P(BMA-*b*-GMA) as the surfactant. In the process of magnetic nanosphere preparation, total Fe content and stirring speed obviously had an effect on the size of the nanosphere. In our experiments, the particle size linearly increased with Fe content. The effect of stirring speed on the size is shown as Figure 6, which indicates that the particle size decreased with increasing stirring speed in the beginning stage. However, the size remained invariable when the stirring speed exceeded 800 rpm.

The magnetic properties of the dried, polymer-coated magnetite nanoparticles were investigated

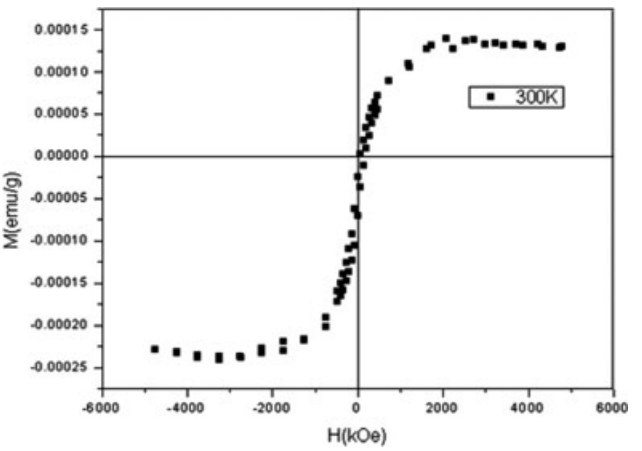

Figure 7 Magnetization curve of a microsphere sample. M is magnetization and H is magnetic intensity.

with vibrating sample magnetometry. Measurements of the magnetite specific magnetization versus applied field yielded qualitatively similar results for all samples. An exemplary data set is shown in Figure 7. It shows a magnetization curve of the nanospheres dispersed in water at room temperature. The particles were essentially superparamagnetic, possessing little hysteresis, which suggested minimal agglomeration of the magnetite nanoparticles. The saturation magnetization was 1.9×10^{-4} emu/g. Because the magnetite content was 5% in this sample, the saturation magnetization per gram of magnetite was 3.8×10^{-3}emu/g. The saturation magnetization of the magnetic nanospheres was lower than that of the bulk materials; however, it was normal for nanoparticles. Typical reasons for this include the reaction or complexation of the surface atoms of the magnetic nanoparticles with surfactant, which may have created a magnetically dead layer.[32] With a significant fraction of surface atoms, any metallic oxide disorder within the surface layer may also lead to a significant decrease in the nanoparticle saturation magnetization.

CONCLUSIONS

ATRP at a lower reaction temperature was used to prepare functional polymers [P(BMA-*b*-GMA)] with narrow distribution. In the presence of sodium hydrogen sulfite, P(BMA-*b*-GMA) was sulfonated in THF at 50°C. The sulfonated P(BMA-*b*-GMA) was used as a surfactant to disperse under vigorous stirring in a selected solvent, which included oil-phase containing P(BMA-*b*-GMA) and magnetite nanoparticles as droplets. Magnetic nanospheres were successfully synthesized. The size of the spheres prepared could be tuned by variation of the preparation conditions, including the stirring speed, copolymer amount, and so on. This allowed us to tune the oil dispersability and magnetic response of the spheres. The magnetic nanospheres exhibited characteristics of superparamagnetism, an absence of hysteresis, remanence, coercivity, and nonsaturation of magnetic moments at room temperature. The saturation magnetization of manganese nanomicroparticles was less than that of their bulk counterparts.

The authors thank Professor Gu (Southeast University) for providing magnetic property measurements.

References

1. Rosensweig, R. E. Ferrohydrodynamics; Cambridge University Press: Cambridge, England, 1985.
2. Kim, D. K.; Zhang, Y.; Voit, W.; Rao, K. V.; Muhammed, M. J Magn Magn Mater 2001, 225, 30.
3. Blum, E.; Cebers, A.; Maiorov, M. M. Magnetic Fluids; de Gruyter: Berlin, 1997.
4. Leslie-Pelecky, D. L.; Rieke, R. D. Chem Mater 1996, 8, 1770.
5. Dailey, J. P.; Phillips, J. P.; Li, C.; Dailey, J. P.; Riffle, J. S. J Magn Magn Mater 1999, 194, 140.
6. Molday, R. S.; MacKenzie, D. J Immunol Methods 1982, 52, 353.
7. Roath, S. J Magn Magn Mater 1993, 122, 329.
8. Jordan, A.; Scholz, R.; Wust, P.; Schbirra, H.; Schiestel, T.; Schmidt, H.; Felix, R. J Magn Magn Mater 1999, 194, 185.
9. Kim, D. K.; Zhang, Y.; Kehr, J.; Klason, T.; Bjelke, B.; Muhammed, M. J Magn Magn Mater 2001, 225, 256.
10. Babes, L.; Denizot, B.; Tanguy, G.; Le Jeune, J. J.; Jallet, P. J Colloid Interface Sci 1999, 212, 474.
11. Papisov, M. I.; Bogdanov, A., Jr.; Schaffer, B.; Nossiff, N.; Shen, T.; Weissleder, R.; Brady, T. J. J Magn Magn Mater 1993, 122, 383.
12. Widder, K.; Flouret, G.; Senyei, A. J Pharm Sci 1979, 68, 79.
13. Gupta, P. K.; Hung, C. T.; Lam, F. C.; Perrier, D. G. Int J Pharm 1988, 43, 167.
14. Ibrahim, A.; Couvreur, P.; Roland, M.; Speiser, P. J Pharm Pharmacol 1982, 35, 59.
15. Iannone, A.; Magin, R. L.; Walczack, T.; Federico, M.; Swartz, H. M.; Tomasi, A.; Vannini, V. Magn Reson Med 1991, 22, 435.
16. Bacri, J.; Perzynski, R.; Salin, D.; Cabuil, V.; Massart, R. J Magn Magn Mater 1990, 85, 27.
17. Khalafalla, S. E.; Reimers, G. W. IEEE Trans Magn 1980, 16, 178.
18. Shen, L.; Stachowiak, A.; Hatton, T. A.; Laibinis, P. E. Langmuir 2000, 16, 9907.
19. Shen, L.; Stachowiak, A.; Seif-Eddeen, K. F.; Laibinis, P. E.; Hatton, T. A. Langmuir 2001, 17, 288.
20. Shimoiizaka, J.; Nakatsuka, K.; Fujita, T.; Kounosu, A. IEEE Trans Magn 1980, 16, 368.
21. Wormuth, K. J Colloid Interface Sci 2001, 241, 366.
22. Pardoe, H.; Chua-Anusorn, W.; St. Pierre, T. G.; Dobson, J. J Magn Magn Mater 2001, 225, 41.
23. Mendenhall, G. D.; Geng, Y.; Hwang, J. J Colloid Interface Sci 1996, 184, 519.
24. Lee, J.; Isobe, T.; Senna, M. J Colloid Interface Sci 1996, 177, 490.
25. Palmacci, S.; Josephson, L.; Groman, E. V. PCT Pat. WO 9505669 (1993).
26. Ding, X. B.; Sun, Z. H.; Wan, G. X.; Jiang, Y. Y. React Funct Polym 1998, 38, 11.
27. Underhill, R. S.; Liu, G. Chem Mater 2000, 12, 2082.
28. Kim, M.; Saito, K. Radiat Phys Chem 2000, 57, 167.
29. Harris, L. A.; Goff, J. D.; Carmichael, A. Y.; Riffle, J. S.; Harburn, J. J.; St. Pierre, T. G.; Saunders, M. Chem Mater 2003, 15, 1367.
30. Pileni, M. P. J Phys Chem 1993, 97, 6961.
31. Greszta, D.; Mardare, D.; Matyjaszewski, K. Macromolecules 1994, 27, 638.
32. Burke, N. A. D.; Stover, H. D. H.; Dawson, F. P. Chem Mater 2002, 14, 4752.